다이렉트릭 혹은 페라이트 물질이 코팅된 도체 실린다에서의 전자파의 산란에 관한 고주파 해석

○김 효 태

포항공과대학

High Frequency Analysis of EM Scattetring from a Circular Conducting Cylinder Coated with Dielectric/Ferrite Material

Hyo Tae KIM

POSTECH

I. INTRODUCTION

A study of electromagnetic scattering and radiation from a conducting surface with dielectric/ferrite coating is of great interest in that it provides an understanding of the effects due to loading on the electromagnetic scattered fields. There is also an emphasis in the design of second generation air-borne vehicles to achieve maximum radar cross section (RCS) reduction by fabricating the structure with radar absorbing material. Therefore, there is a strong need for an analytical tool to predict the electromagnetic scattered field from a dielectric/ferrite coated conducting surface. Although an efficient approximate uniform GTD solution has been obtained for the EM scattering from a smooth perfectly conducting convex surface surface [1,2], no such solution exists for a conducting surface covered with dielectric/ferrite material. As a first step leading to the problem of the scattering from coated convex surface, we develop an approximate GTD solution for the EM scattering from a circular cylinder with dielectric/ferrite coating. The solution is convenient for the engineering application due to its simple ray format. The ray paths associated with the solution for the perfectly conducting cylinder [1] remain unchanged for the coated cylinder. Some typical numerical results for the field pattern are also presented in this paper.

II. THE CANONICAL PROBLEM

As illustrated in Figure 1, a coated cylinder with radius b is excited by a line source directed parallel to the cylinder axis (z-axis). The source is either an of electric current filament I (TM case) or magnetic current filament K (TE case). Both the source and the field point are assumed to be located outside the coated cylinder. The coating has a thickness d = b - a and is homogeneous with permittivity ϵ_1 and permeability μ_1, both of which may be complex. The two-dimensional Green's function satisfies the equation

$$\left[\frac{1}{\rho}\frac{\partial}{\partial\rho}\rho\frac{\partial}{\partial\rho}+\frac{1}{\rho^2}\frac{\partial^2}{\partial\phi^2}+k_o^2\right]G(\vec{\rho},\vec{\rho}')=\frac{-\delta(\rho-\rho')\,\delta(\phi-\phi')}{\rho}$$

subject to the boundary conditions at ρ = a and ρ = b and the radiation condition at $\rho=\infty$. For excitation by a line source of electric current, we have (for $e^{j\omega t}$ time variation)

$$E_z=-j\omega\mu_o IG,$$

and for the magnetic line source, we have

$$H_z=-j\omega\epsilon_o KG,$$

The angular eigenfunction series solution for the problem can be obtained as

$$G(\rho,\phi)=\frac{-j}{8}\sum_{n=-\infty}^{\infty}H_n^{(2)}(k_o\rho_>)\left[H_n^{(1)}(k_o\rho_<)+F_n(n)H_n^{(2)}(k_o\rho_<)\right]e^{-jn\phi}$$

where

$$F_e(n)=-\frac{H_n^{(1)'}(k_ob)-jC_e(n)H_n^{(1)}(k_ob)}{H_n^{(2)'}(k_ob)-jC_e(n)H_n^{(2)}(k_ob)}$$

$$F_h(n)=-\frac{H_n^{(1)'}(k_ob)-jC_h(n)H_n^{(1)}(k_ob)}{H_n^{(2)'}(k_ob)-jC_h(n)H_n^{(2)}(k_ob)}$$

where

$$C_e(n)=-j\frac{Z_o}{Z_1}\cdot\frac{H_n^{(1)'}(k_1b)H_n^{(2)}(k_1a)-H_n^{(2)'}(k_1b)H_n^{(1)}(k_1a)}{H_n^{(1)}(k_1b)H_n^{(2)}(k_1a)-H_n^{(2)}(k_1b)H_n^{(1)}(k_1a)}$$

$$C_h(n)=-j\frac{Z_1}{Z_o}\cdot\frac{H_n^{(1)'}(k_1b)H_n^{(2)'}(k_1a)-H_n^{(2)'}(k_1b)H_n^{(1)'}(k_1a)}{H_n^{(1)}(k_1b)H_n^{(2)'}(k_1a)-H_n^{(2)}(k_1b)H_n^{(1)'}(k_1a)}$$

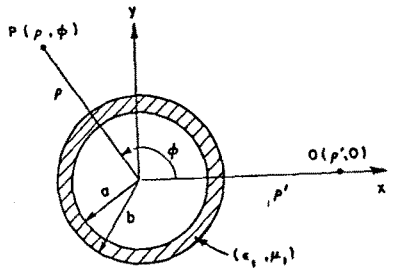

Fig 1. Geometry of the problem

III. GTD SOLUTION

The angular eigenfunction solution is very slowly convergent when the radius of the cylinder is large in terms of the wave length. Furthermore, the physical interpretation of the scattering mechanism is not possible from the eigenfunction solution. Ray optical solution for the problem can be obtained by taking the same procedure as that for the perfectly conducting cylinder. First, the field representation in the angular eigenfunction series is transformed into the integral form. The GTD ray solution is the result of asymptotic evaluation of the integral. It is noted that the behavior of high-frequency field is characterized by geometric optical domains. Thus, a separate analysis is given for the lit region and the shadow region.

It can be shown that the integral form of $G(\rho,\phi)$ can be decomposed into two terms

$$G(\rho,\phi) \equiv u = u^o + u^{cw}$$

where

$$u^o = \frac{-j}{8}\int_{-\infty-j\tau}^{\infty-j\tau} H_\nu^{(2)}(k_o\rho_>)\left[H_\nu^{(1)}(k_o\rho_<) + F_{s,h}(\nu)H_\nu^{(2)}(k_o\rho_<)\right]e^{-j\nu\phi}\,d\nu$$

$$u^{cw} = \frac{-j}{8}\int_{-\infty-j\tau}^{\infty-j\tau} H_\nu^{(2)}(k_o\rho_>)\left[H_\nu^{(1)}(k_o\rho_<) + F_{s,h}(\nu)H_\nu^{(2)}(k_o\rho_<)\right] \times \frac{e^{-j\nu(2\pi+\phi)} + e^{-j\nu(2\pi-\phi)}}{1-e^{-j2\nu\pi}}\,d\nu$$

A) Geometric Optical Field

Lit region is in the angular range of $0 \le \phi < \phi_{sb}$, where the field point is in the line of sight from the source. After the Hankel functions in the integrant are replaced by the Debye approximations forms, u^o in the integral form is evaluated asymptotically via the stationary phase method. Casting the result into the ray format leads to geometric optical fields (i.e. incident field u^i and reflected filed u^r). The direct incident ray from the source is given as

$$u^i \approx \frac{e^{-j\frac{\pi}{4}}}{2\sqrt{2\pi}}\frac{e^{-jk_o l}}{\sqrt{k_o l}} \qquad for \quad 0 \le \phi < \phi_{sb}$$

The field reflected on the cylinder surface can be expressed as

$$u^r = u^i(Q)\cdot R_{s,h}\cdot S_p\, e^{-jk_o l_2} \qquad 0 \le \phi < \phi_{sb}$$

The usual spreading factor S_p associated with the reflection from the curved surface is

$$S_p \equiv \sqrt{\frac{l_1 b\cos\theta_i}{2l_1 l_2 + (l_1+l_2)b\cos\theta_i}}$$

The reflection coefficient R is given as

$$R_s = -\frac{Z_o - jZ_1\cos\theta_i/\cos\theta_t\ \tan\{\Psi(a,b,k_1)\}}{Z_o + jZ_1\cos\theta_i/\cos\theta_t\ \tan\{\Psi(a,b,k_1)\}}$$

for TMz case

$$R_h = \frac{Z_o - jZ_1\cos\theta_t/\cos\theta_i\ \tan\{\Psi(a,b,k_1)\}}{Z_o + jZ_1\cos\theta_t/\cos\theta_i\ \tan\{\Psi(a,b,k_1)\}}$$

for TEz case

where

$$\Psi(a,b,k_1) \equiv k_1(b\sin\beta_b - a\sin\beta_a) - k_o b(\beta_b - \beta_a)\sin\theta_i$$

$$\sin\beta_b = \cos\theta_t = \sqrt{1-\left(\frac{k_o}{k_1}\sin\theta_i\right)^2}$$

$$\sin\beta_a = \sqrt{1-\left(\frac{b}{a}\sin\theta_t\right)^2} = \sqrt{1-\left(\frac{k_1 b}{k_o a}\sin\theta_i\right)^2}$$

For a thin coating case,

$$\Psi(a,b,k_1) \approx k_1(b-a)\sin\beta_a = k_1 d\cos\theta_t$$

Therefore, the reflection coefficient can be reduced to the well-known reflection coefficient for a planar grounded slab with a plane wave incidence.

$$R_s = -\frac{Z_o - jZ_1\cos\theta_i/\cos\theta_t\ \tan(k_1 d\cos\theta_t)}{Z_o + jZ_1\cos\theta_i/\cos\theta_t\ \tan(k_1 d\cos\theta_t)}$$

$$R_h = \frac{Z_o - jZ_1\cos\theta_t/\cos\theta_i\ \tan(k_1 d\cos\theta_t)}{Z_o + jZ_1\cos\theta_t/\cos\theta_i\ \tan(k_1 d\cos\theta_t)}$$

The ray paths asociated with the incident and the reflected field are illustrated with Figure 2.

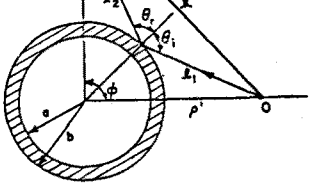

Fig 2. Geometric optical field

B) Creeping Wave Diffraction

Field in the shadow region is entirely associated with the creeping wave which propagates azimuthally on the cylinder surface and carries the electromagnetic energy into the showdow region. The creeping diffraction can be obtained from the residue series solution for the integral representation of the field. The residue series solution is fast convergent. For the perfectly conducting cylinder, the contribution of the first creeping wave mode to the diffracted field is always dominant over other higher modes. However this is not always true for the coated cylinder.

The ray format for the creeping wave diffraction is given as

$$u^d \approx u^i(Q_1)\cdot \mathcal{D}_n^{s,h}(Q_1)\cdot e^{-j\nu_n\theta}\cdot \mathcal{D}_n^{s,h}(Q_2)$$

$$= u^i(Q_1)\cdot \mathcal{D}_n^{s,h}(Q_1)\cdot e^{-(\alpha_n'+j\beta_n')l}\cdot \mathcal{D}_n^{s,h}(Q_2)$$

where

$$\mathcal{D}_n^{s,h}(Q) = \left[\sqrt{\frac{2}{\pi}}\cdot\frac{4}{k_0 b}\cdot\frac{e^{-j\frac{3\pi}{4}}}{H_{\nu_n}^{(2)}(k_0 b)\frac{\partial}{\partial\nu}\left[H_\nu^{(2)'}(k_0 b)-jC_{s,h}(\nu)H_\nu^{(2)}(k_0 b)\right]_{\nu=\nu_n}}\right]^{\frac{1}{2}}$$

The complex azimuthal propagation constants ($\alpha_n'+j\beta_n'$) of the creeping wave modes are determined from the roots of the transcendental equation given as

$$H_\nu^{(2)'}(k_0 b) - jC_{s,h}(\nu)H_\nu^{(2)}(k_0 b)\Big|_{\nu=\nu_n} = 0$$

$$\alpha_n' = -Im\left[\frac{\nu_n}{b}\right] \quad ; \quad \beta_n' = Re\left[\frac{\nu_n}{b}\right]$$

The ray picture for the creeping wave diffraction is given in Figure 3. Typical trajectories of the propagation constants for several coating materials are also plotted in Figure 4.

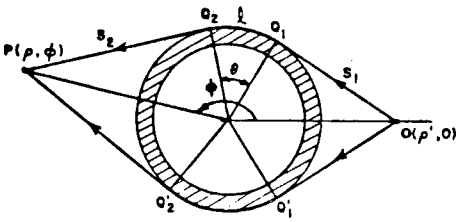

Fig 3. Creeping wave diffraction

Asymptotic evaluation for U^{LW} can be obtained by the same procedure. Physically, $U^{C.W}$ represents the multiple encirclements of the creeping wave. It can be shown that $U^{C.W}$ consists of two terms: the first term represents multiple encirclements in the counterclockwise sense and the second term represents those in the opposite direction.

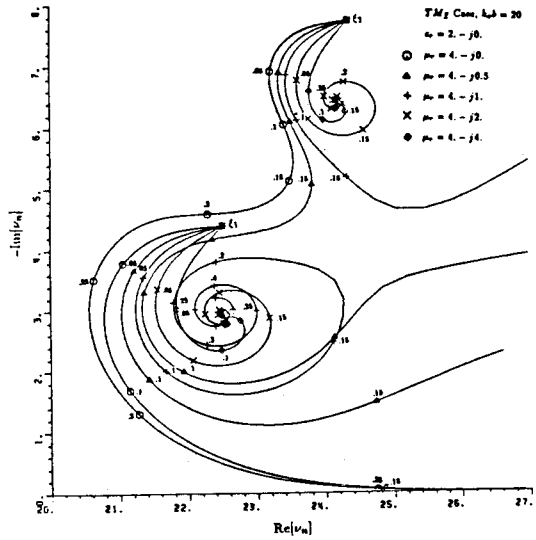

Fig 4. Propagation constant

VI. NUMERICAL RESULTS AND CONCLUSION

The numerical results of the obtained GTD solution as illustrated in Figure 5 -10 show excellent agreements with the angular eigenfunction results in the deep lit region and the deep shadow region. However, as expected, the GTD solution fails within the shadow boundary (SB) transition region. For the unifom result in the transition region, a more complicated analysis should be performed.

V. REFERENCE

[1] P.H. Pathak, "An asymptotic analysis of the scattering of plane wave by a smooth convex cylinder", Radio Science, Vol 14. No. 3, 1979.

[2] P.H. Pathak, W.D. Burnside and R.J. Marhefka, "A uniform GTD analysis of the diffraction of the electromagnetic waves by a smooth convex surface". IEEE Trans. on Antennas & Propagation, AP-28, No. 5, Sep. 1980.

[3] N. Wang and H.T. Kim, "UTD solution for the electromagnetic scattering from a circular cylinder with a constant surface impedance", Technical Report 716495-2, Office of Naval Weapons Center, Oct. 1985.

[4] J.R. Wait and A.M. Conda, "Diffraction of the electromagnetic waves by smooth obstacles for grazing angles", J. Res. Nat. Bur. Stand. 63D(2), pp 181-197, Sep.-Oct. 1959

[5] N. Wang, "Electromagnetic scattering from a dielectric coated cylinder", IEEE Trans. on Antennas & Propagation, AP-33, No. 9, Sep. 1985.

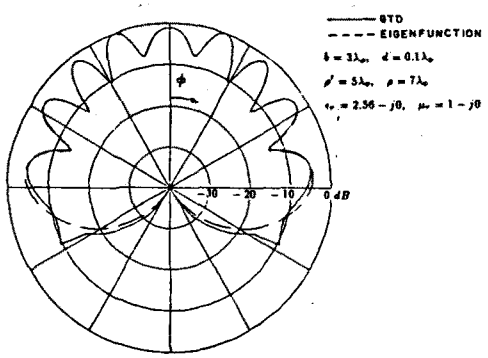

Fig 5. Normalized bistatic scattering pattern TMz Case

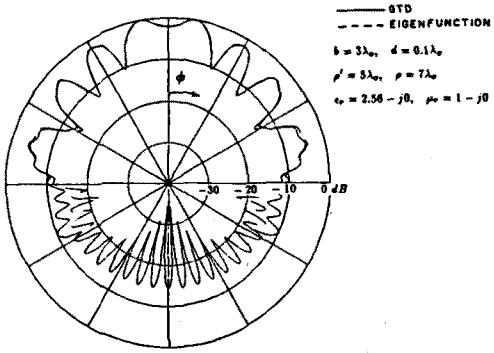

Fig 6. Normalized bistatic scattering pattern TEz Case

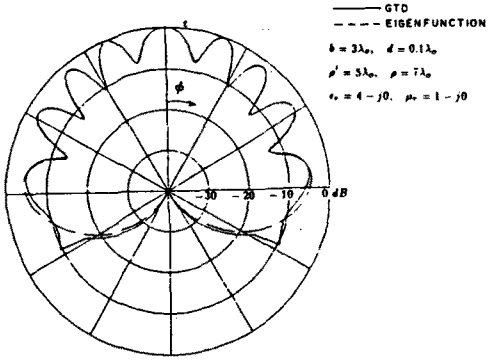

Fig 7. Normalized bistatic scattering pattern TMz Case

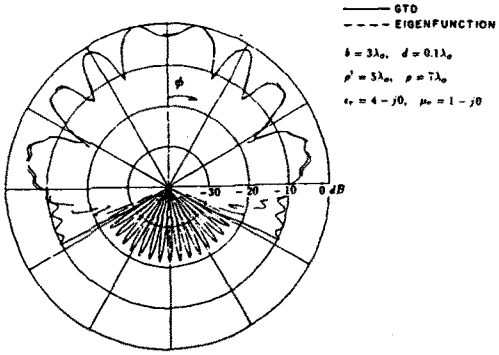

Fig 8. Normalized bistatic scattering pattern TEz Case

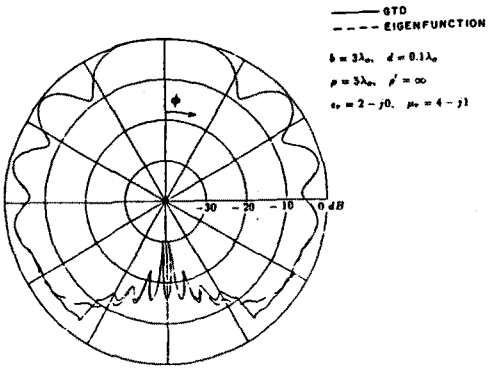

Fig 9. Normalized bistatic scattering pattern TMz Case

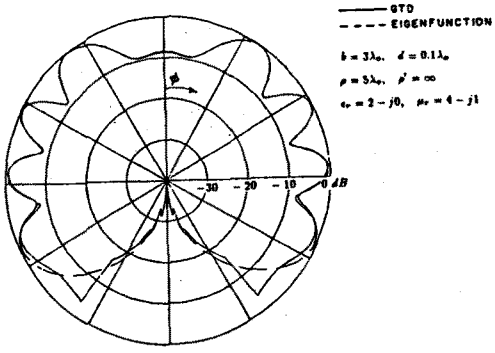

Fig 10. Normalized bistatic scattering pattern TEz Case